Extending the autonomy time of an icelined solar powered vaccine cooler

Jensen, Jonas K.; Busk, Christoffer; Cording, Claus ; Pedersen, Per Henrik ; Markussen, Wiebke Brix

Published in:
Proceedings of the 25th IIR International Congress of Refrigeration

Link to article, DOI:
10.18462/iir.icr.2019.1006

Publication date:
2019

Document Version
Peer reviewed version

Manuscript ID: 1006
DOI: 10.18462/iir.icr.2019.1006

Extending the autonomy time of an icelined solar powered vaccine cooler

Jonas K. JENSEN [(a)], Christoffer BUSK [(a)], Claus CORDING [(c)], Per Henrik PEDERSEN[(b)], Wiebke B. MARKUSSEN[(a)]

[(a)] Department of Mechanical Engineering, Technical University of Denmark
Kgs. Lyngby, 2800, Denmark, jkjje@me.dtu.dk
[(b)] Danish Technological Institute
Taastrup, 2630, Denmark, prp@mek.dtu.dk
[(c)] Vestfrost Solutions A/S
Esbjerg, 6705, Denmark, info@vestfrostsolutions.com

ABSTRACT

The autonomy time of an icelined solar powered vaccine cooler expresses the amount of hours the cooler is able to keep vaccines within an acceptable temperature range during low solar radiation conditions, i.e. when the compressor of the cooling system is idle. This study investigates how different parameters related to the cooler cabinet and ice storage affect the autonomy time. A dynamic model of the vaccine cooler cabinet including the ice storage was used for the investigation. The model was calibrated using measurements from three different experimental setups, and the calibrated model showed a good agreement with the measurements. The results show that the mass of ice in the storage was the most promising parameter to consider for prolonging the autonomy time. Furthermore, it was shown that reduction of the thermal bridges in the cabinet also is of great importance.
Keywords: Icelined Refrigerator, Autonomy Time, Solar Powered Refrigeration, Vaccine Cooler, WHO.

1. INTRODUCTION

In many developing countries, the electrical grid is either unreliable or not existing, especially in the rural regions and small villages. A study by Adair-Rohani (2013) showed that 25 % of health facilities in Sub-Saharan Africa did not have access to any kind of electricity. Furthermore, 1/3 of hospitals in the area experienced unreliable grid connections. This leads to limited use of electrical applications, such as cooling systems for of medical supplies and products.
Medical supplies such as vaccines are critical in the developing countries. According to the World Health Organization (WHO), the global immunization coverage, i.e. the amount of people with effective vaccines in their blood, has stalled at around 85 % (WHO, 2018) and only very limited progress was attained over the last years. It is stated that 1.5 million lives could be saved if the global immunization coverage improves.
One reason for the fading progress is that vaccines need to be stored cold, in order to avoid spoilage and loss of potency. According to WHO (2015) vaccines should be kept at a storage temperature between 2 °C and 8 °C at all times from manufacturing to administration, in order to ensure the quality of the vaccines. Keeping vaccines cold in rural regions of developing countries is complicated, due to the lack of reliable electricity, as well as challenging ambient conditions in terms of both temperature and humidity.
To solve this issue several commercial coolers exists, which are able to operate without a grid connection. These coolers typically use photovoltaic (PV) modules for power supply and either a battery or an ice bank for energy storage.

1.1. Literature Review

Fatemulla (2011), investigated a refrigeration system using PV modules and a battery for energy storage. The study focused on comparing the costs of using PV, rather than conventional grid

electricity. They found that a payback period of around 7 years was expected from the PV modules. Since this was shorter than the expected lifetime, the authors deemed PV a viable investment.
Several studies have investigated the use of thermoelectric coolers for off-grid cooling purposes (Hans et al., 2016, Wang et al. 2011). Hans et al. (2016) investigated a thermoelectric cooler driven by a PV and with a battery for storage. Through experimental testing, they found that the cooler was able to keep the cold room temperature within the defined boundaries of 10-15 °C, while operating with a coefficient of performance (COP) of 0.34.
Aktacir (2011) also considers a refrigerator powered by a PV / battery combination. The system performance on a daily, as well as a seasonal level was investigated for one of the warmest regions of Turkey. It is found that the PV solution was able to deliver the required amount of energy needed to operate the refrigerator at desired conditions.
As stated in Pedersen et at. (2019) experience has shown that the use of batteries in vaccine coolers often is related to increased costs, since the life-time of the batteries is suffering from the high ambient temperatures and the frequent deep discharging. This encouraged the development of direct drive solar powered vaccine coolers with ice storage. Since PV modules generate direct current (DC), it is often advantageous to use a DC compressor for the refrigeration system. In this way the compressor may be connected directly to the PV panels, as a so-called direct drive compressor.
In a study by Ekren (2013), such a DC compressor was investigated, to see if the energy usage could be reduced by use of a variable speed controller, rather than an on/off controller. It was found that the use of variable speed control leads to an increase in COP as well as exergetic efficiency, particularly at high rotation speeds.
In Jensen et al. (2019) three different compressor control strategies were investigated for two different direct drive compressors. Through numerical modelling it was found that by selecting an appropriate compressor control strategy the amount of PV panels needed to operate a vaccine cooler could be halved if the compressor start power could be supplied by e.g. a capacitor or a smart start algorithm.
Pilatte (1984) investigated a refrigerator powered by PV cells, which had the ability to produce ice and use this for energy storage. The cooler was relatively large, with a vaccine storage chamber of 70 litres, and an additional storage room of 70 litres, with a temperature of about 10 °C. The ice-storage of 14 litres was able to produce 2 kg of ice within 24 hours. Performing several tests revealed that the cooler was able to deliver the requirements set by the WHO for vaccine coolers in tropical regions. During operation, the cooler had an average energy consumption of 370 Wh within 24 hours and by using a high level of thermal insulation COPs as high as 1.6 were measured.
Walker (2007) investigated how to design a low-cost vaccine cooler, focusing on a heat transfer regulating device, whose purpose is to control the temperature within the vaccine storage chamber. This cooler also utilized an ice storage. Through modelling of the system, the temperature response of the vaccine chamber due to openings of the cooler lid was investigated. It was found that even though only one vial is present, and the entire cooler is filled with air at 45 °C, the single vial still remained within the boundary of the acceptable temperature range.

1.2. Scope

Autonomy time of a vaccine cooler, as defined by WHO, is the number of hours the vaccine cooler can keep the vaccines within the acceptable temperature range during low solar radiation conditions, i.e. lower than what is required for the compressor to run, but low-consumption equipment such as fans or electronics might be operating. A measurement of the autonomy time starts when the compressors shuts off and ends once a single temperature measurement of the vaccines reaches a temperature of 8 °C. In the present study we focus on extending the autonomy time of vaccine coolers using ice storage. By use of numerical analysis, we investigate how different parameters of the ice storage and cabinet affect the autonomy time of the vaccine cooler.

2. METHODS

In order to investigate the autonomy time of a vaccine cooler a dynamic model of the cabinet including the ice storage was created. The model was implemented in Engineering Equation Solver (Klein, 2018).

2.1. Cabinet Model

Fig. 1 (left) shows a sketch of the considered vaccine cooler layout. The sketch is a cut through the middle of the vaccine cooler and it should be noted that the ice-storage surrounds the four side walls of the vaccine compartment. Furthermore, the evaporator is a spiral-shaped pipe, wrapped around the ice-storage. The condenser is also a long pipe, but placed on one side of the unit, similarly to a household refrigerator. The ice-storage itself is placed in the top part of the side wall and separated of the vaccine chamber by the frame with a thin layer of plastic material between the frame and the ice-storage. All walls are insulated with PU foam as well as a vacuum insulation panel on the outside of the insulation. The vaccine cooler also contains a lid, which is insulated by PU foam.
For the modelling the condenser and evaporator tubes were disregarded, since the refrigeration system is idle during autonomy time. The vaccine cooler was divided into eight control volumes as seen in Fig. 1 (right). The arrows indicate how a given control volume interacts with the neighbouring control volumes. Red arrows indicate heat transfer by convection, calculated by multiplying a convective heat transfer coefficient with the heat transferring area and the temperature difference between the surface and the ambient or cabinet inside air temperature.

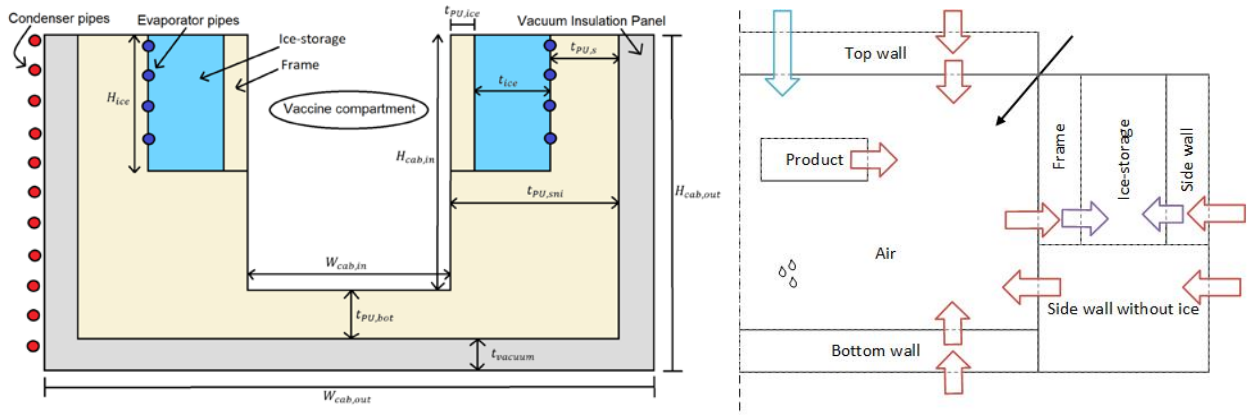

Figure 1: (Left) Sketch of the vaccine cooler cabinet with ice storage. (Right) Sketch of the modelled control volumes and their interactions

The two purple arrows indicate heat transfer by conduction. The blue arrow indicates heat transfer through thermal bridges. This was modelled by fixing a UA-value for the thermal bridges and multiplying this with the temperature difference between the ambient air and the air inside the vaccine compartment. Air infiltration, indicated by the solid black arrow in Fig. 1, was taken into account in the energy balance of the air control volume as well as possible condensation of moist air, as indicated by the water droplets in the figure.
Dynamic mass and energy balances were formulated for all control volumes. For the air, product and ice-storage control volumes a lumped capacitance approach was chosen, while transient conduction through a composite wall was applied for the wall and frame insulation control volumes. The walls consisted of an outer layer of steel, a vacuum insulation panel, a layer of insulation material (PU-foam) and another layer of steel on the inside. The walls were discretised such that a calculation node was placed at each material interface and additionally 10 nodes were placed inside the layer of PU foam.
The frame consisted of an aluminium layer, a thin layer of insulation material and another aluminium layer. Since the insulation material only a thin layer only 3 nodes were added in this layer. Furthermore, a contact resistance of 500 W $m^{-2}K^{-1}$ between the ice and the aluminium layer was defined.
The product consisted of a number of vials. Each vial was assumed to have a cylindrical shape. The density and heat capacity of the vials was assumed to be similar to liquid water.

2.2. Ice Bank Storage

The ice bank storage was able to interact with the frame and the side wall. The model was built such that both freezing and thawing of the ice could be simulated. Since the water is placed in a closed and stable container some degree of subcooling of the liquid is experienced prior to freezing and the water will be at a metastable state until it reaches the freezing point. For the simulations the freezing

point temperature was a user input, based on experiences from experimental tests. The properties of the subcooled water were considered similar to non-sub-cooled liquid water. When reaching the

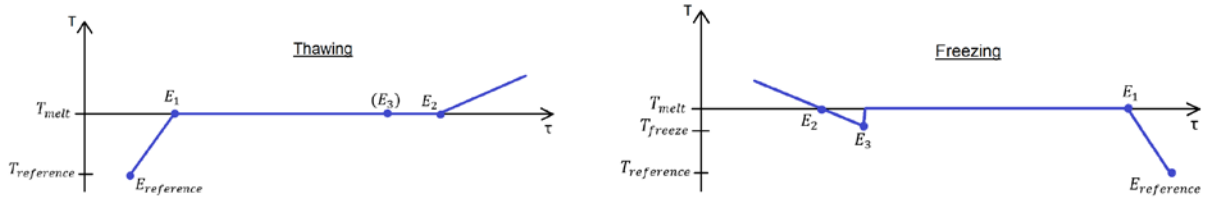

Figure 2: Temperatures and energy levels in the ice-storage during freezing and thawing

freezing point temperature, part of the ice would freeze rapidly and the temperature would instantly increase to 0 °C. Figure 2 sketches the assumed temperature course during freezing and thawing. A reference temperature was defined at -15 °C. This reference temperature was used for calculating reference levels of internal energy of the ice:

$$E_{\text{reference}} = M_{\text{ice}} \cdot u(T_{\text{reference}}, p) \quad \text{Eq. (1)}$$

$$E_1 = E_{\text{reference}} + M_{\text{ice}} \cdot c_{\text{ice}} \cdot (T_{\text{melt}} - T_{\text{reference}}) \quad \text{Eq. (2)}$$

$$E_2 = E_1 + M_{\text{ice}} \cdot \Delta h_{fs} \quad \text{Eq. (3)}$$

$$E_3 = E_2 - M_{\text{ice}} \cdot c_{\text{water}} \cdot (T_{\text{melt}} - T_{\text{freeze}}) \quad \text{Eq. (4)}$$

By comparing the changes in internal energy of the ice calculated from the dynamic energy balance to the energy levels, E_1, E_2 and E_3 the current temperature and ice fraction was calculated. The melting point temperature, T_{melt}, was set to 0 °C, while the freezing point temperature, T_{freeze}, was set to -6 °C.

2.3. Calibration

As a first step a calibration of the model was carried out. The parameters fixed in the calibration were:

- The UA-value representing the losses through thermal bridges in the cabinet
- The convective heat transfer coefficient on the inside of and outside of the cabinet

It was assumed that the heat transfer coefficient on the outside of the cabinet was equal to the heat transfer coefficient on the inside of the cabinet, and also the heat transfer coefficient between the product and the air was assumed equal to the heat transfer coefficient between the inside wall and the air. For the calibration the simulated results were compared to test results from autonomy time measurements of three different test setups using the considered vaccine cooler cabinet. Apart from the autonomy time also the steady state temperature was used as a target parameter. The steady state temperature denotes the temperature of the air, when the entire system is in a steady state condition during phase change in the ice-storage.

One of the tests was carried out according to the WHO performance quality and safety (PQS) standard at hot zone conditions, i.e. an ambient temperature, T_{amb} = 43 °C (WHO, 2010). According to the test standard, 1/5 of the nominal cabinet volume should be filled with water packages, each package containing 0.4 kg of water, which corresponded to 4.4 kg for the considered cabinet. For the simulations a single volume of water was assumed. The second test was carried out by the Danish Technological Institute (DTI), at temperate zone conditions i.e. T_{amb} = 32 °C. In this test the hold-over time was measured instead of the autonomy time. This meant that the measurement was carried out until the vaccines reached a temperature of 12 °C in stead of 8 °C, which was the case for the two other tests. The product inside the cooler cabinet was one test package Tylose gel of 0.5 kg. The last test was carried out at DTU. In this test the ambient conditions were not controlled, and the average ambient temperature in the lab during measurements was 22.1 °C. In this test the cabinet was empty during measurements and the time was stopped when the air inside the cabinet reached 8 °C.

2.4. Simulated Cases

A baseline model was established using geometrical data from the considered vaccine cooler cabinet and values of the convective heat transfer coefficient and UA-value representing the thermal bridges obtained from the calibration procedure. Taking this baseline model as a reference, the following parameters were varied in order to investigate their impact on the autonomy time and steady state temperature:

- The height of the ice bank. In this case the mass of ice was kept constant, while the thickness of the ice bank was changed as a function of the height.
- The mass of the ice. The thickness of the ice storage was held constant while the height was changed to give room for extra mass.
- The thickness of the PU insulation. For this case the inner dimensions of the cabinet were held constant while extra insulation was added on all walls.
- The UA-value of the thermal bridges.

3. RESULTS

3.1. Model Calibration

By running the model with different combinations of the convective heat transfer coefficient and the overall heat transfer coefficient representing the thermal bridges, the best combination of parameter values was found using the values stated in Table 1.

Table 1. Values of calibrated parameters

Convective heat transfer coefficient, W m^{-2} K^{-1}	7
UA-value of thermal bridges, W K^{-1}	0.26

Using the baseline model including the values presented in Table 1 and input parameters for ambient conditions corresponding to the three different measurement environments, simulated autonomy times were found as seen in Table 2. The simulated autonomy times corresponded well with the measurements, showing discrepancies of less than 3 %. Apart from the autonomy time also the steady state temperatures are shown in Table 2. As seen the steady state temperature during simulations corresponded very well with the measured temperatures.

Table 2. Comparison of autonomy time and steady state temperature of the air for measurements and simulations with the calibrated model

	Measured h	Simulated h	Deviation h	Deviation %
WHO	72.4	74.5	2.1	2.9
DTI	111.3	111.6	0.3	0.3
DTU	156.4	154.3	2.7	1.7
	Measured °C	Simulated °C	Deviation °C	
WHO	5.8	5.8	0.0	n/a
DTI	4.3	4.2	0.1	n/a
DTU	3.0	2.9	0.1	n/a

3.2. Extending Autonomy Time

In Fig. 3 (left) the autonomy time and steady state temperature of the air inside the cabinet is shown as a function of the ice bank height for two different ambient temperatures. The mass of ice was kept constant in this case, which meant that the ice bank thickness was decreasing with added height. As seen the autonomy time decreases slightly with increasing height for both 32 °C and 43 °C ambient temperature. At the same time the steady state temperature was found to decrease. By increasing the ice bank height also the area between air and frame is increased, which results in an increased convective heat transfer from this surface, and the air temperature thus decreases. The lower air temperature inside the cabinet then results in larger heat losses through the outer walls which causes the decrease in autonomy time. At an ambient temperature of 32 °C the steady state temperature of the air got below the lower limit 2 °C when increasing the ice bank height by 18 cm. Fig. 3 (right) shows the autonomy time and steady state temperature as a function of the ice bank mass. In this case the height of the ice bank was also increased while the thickness was kept constant. In this

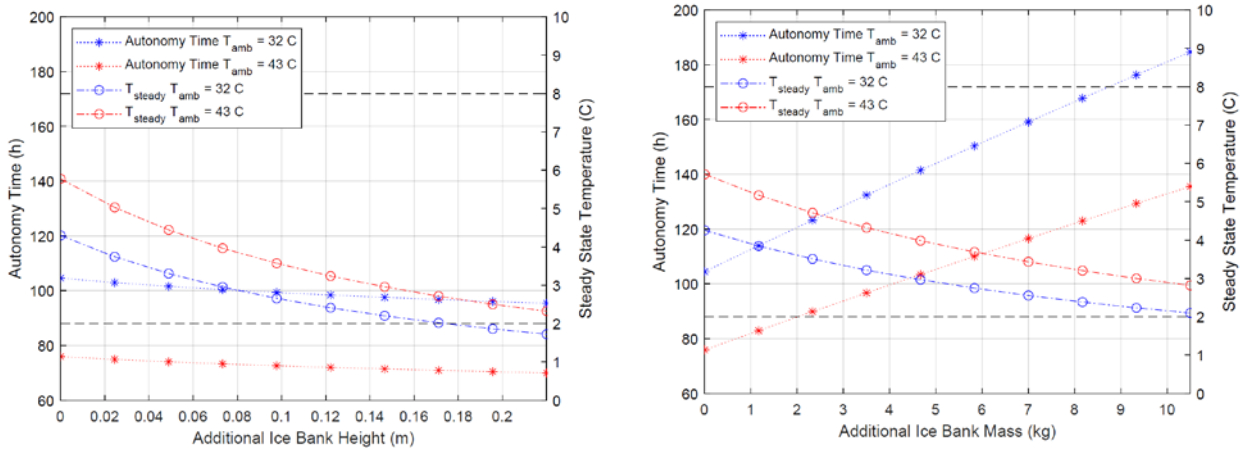

Figure 3: Autonomy time and steady state temperature as a function of additional ice bank height (left) and additional ice bank mass (right) compared to the baseline model

case the autonomy time increases significantly with added mass of the ice. This trend was expected as added mass in the ice bank means a larger storage capacity. Adding 10 kg of ice to the storage of the reference model resulted in around 80 % increase in autonomy time for both ambient temperatures. The steady state temperatures show a similar decrease as for the case where height is increased with constant the ice bank mass, however, staying within the limits, above 2 °C.
Fig. 4 (left) shows the autonomy time and steady state temperature as a function of added PU-insulation in all outer cabinet walls. As seen the autonomy time increases slightly with increasing

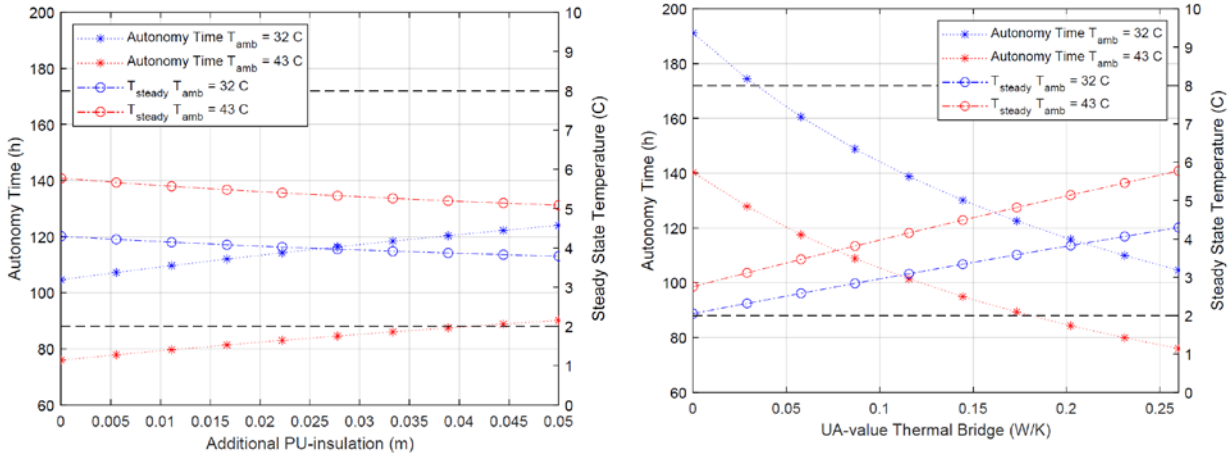

Figure 4: Autonomy time and steady state temperature as a function of additional PU-insulation in the cabinet walls (left) compared to the baseline model and as a function of the UA-value of the thermal bridges (right)

insulation thickness. Increasing the insulation thickness of the outer walls reduces the convective heat loss through the walls, which leads the increase in autonomy time. Adding extra 5 cm to the insulation of the outer walls increases the autonomy time by 10 to 20 % depending on the ambient temperature. The steady state temperature is mainly governed by the insulation thickness between the ice storage and the vaccine chamber, and therefore only changing less than 1 °C, when adding 5 cm to the insulation thickness of the outer walls.
In Fig. 4 (right) the UA-value of the thermal bridges was varied between 0 WK^{-1}, meaning no losses due to thermal bridges, up to 0.26 WK^{-1}, which was the value found from the calibration of the baseline model. For a cabinet without thermal bridges autonomy times of 190 h and 140 h were obtained for ambient temperatures of 32 °C and 43 °C, respectively. Removing all thermal bridges thus has almost the same impact on the autonomy time as adding 10 kg of ice to the ice to the ice storage. Also the steady state temperatures are significantly influenced by the thermal bridges. At an ambient temperature of 43 °C the steady state temperature decreases from 5.8 °C to 2.9 °C when removing the thermal bridges, and at an ambient temperature of 32 °C the steady state temperature decreases from 4.2 °C to 2.0 °C, which is at the limit of the acceptable air temperature inside the cabinet.
For the solar powered vaccine cooler a longer autonomy time means a less vulnerable system in periods with low solar radiation. For extending the autonomy time, the results presented in Figure 3 and Fig. 4 suggest that focus is put on increasing the mass of the ice storage and reducing the thermal bridges of the cabinet.

4. DISCUSSION

The model showed good agreement with measured values of the autonomy time, when using the calibrated values of the heat transfer coefficient and UA-value of the thermal bridges. Considering the UA-value of the thermal bridges the results showed that both the autonomy time and the steady state temperature were quite sensitive to the chosen value. A more thorough analysis of the thermal bridges therefore seems relevant for future work. Considering the convective heat transfer coefficient, the same value was used for calculating the heat transfer on the inside wall, the outside wall and between the product and the air. Due to different geometries, air flow conditions and different temperature levels it is expected that the heat transfer coefficients would not be equal in reality. A refinement of the convective heat transfer coefficients could possibly lead to a more realistic model, however this would also increase the number of parameters to be calibrated.
For the air, ice and product control volumes it was assumed that the lumped capacitance method could be applied. In reality temperature gradients are expected in all three control volumes. A sensitivity analysis calculating the Biot number for different combinations of convective heat transfer coefficients and ice storage thicknesses relevant in this study, showed that the Biot numbers were close to 0.1, which is usually seen the limit of the validity of the lumped capacitance method. Furthermore, as soon as the ice starts to melt and the ice storage is filled with an increasing amount of liquid water natural convection will occur inside the ice storage, which is not accounted for in the current model. Natural convection on the water side will decrease the resistance and might thus decrease the expected autonomy time.

5. CONCLUSIONS

A dynamic model of an ice-lined vaccine cooler cabinet was used to investigate the autonomy time and the steady state temperature of the air during phase change of the ice. A baseline model representing an existing cabinet was calibrated against experimental results from three different measurement setups. The calibrated baseline model showed a good agreement with the measurements. It was investigated how different parameters related to the cooler cabinet and ice storage affected the autonomy time, while making sure that the steady state temperature stayed in an the acceptable range between 2 °C and 8°C. The results showed that the mass of ice in the storage was the most promising parameter to consider for prolonging the autonomy time. Furthermore, it was shown that a reduction of the thermal bridges in the cabinet also is of great importance.

ACKNOWLEDGEMENTS

This research project is financially funded by EUDP (Energy Technology Development and Demonstration). Project title: "Second Generation Solar Direct Drive Refrigerators", project number: 64017-0556

NOMENCLATURE

c	Specific heat (J kg^{-1} K^{-1})	p	pressure (kPa)
E	Internal energy level (J)	T	temperature (K)
M	mass (kg)	u	Specific internal energy (J/kg)

REFERENCES

Adair-Rohani, H., Zukor, K., Bonjour, S., Wilburn, S., Kuesel, A.C., Hebert, R., Fletcher, E.R., 2013. Limited electricity access in health facilities of sub-Saharan Africa: a systematic review of data on electricity access, sources, and reliability. Global Health: Science and Practice 1 (2) 249-261.

Aktacir, M.A., 2011. Experimental study of a multi-purpose PV-refrigerator system. International Journal of Physical Sciences 6(4):746-757.

Ekren, O., Celik, S., Noble, B., Krauss, R., 2013. Performance evaluation of a variable speed dc compressor. International Journal of Refrigeration 36(3),745-757.

Fatehmulla, A., Al-Shammari, A.S., Al-Dhafiri, A.M., and Al-Bassam A.A., 2011. Design of energy efficient low power PV refrigeration system. In Electronics, Communications and Photonics Conference (SIECPC), 2011 Saudi International, pages 1-5. IEEE.

Hans R., Kaushik S.C., Manikandan, S., 2016. Experimental study and analysis on novel thermo-electric cooler driven by solar photovoltaic system. Applied Solar Energy 52 (3) ,205-210.

Jensen, J.K., Moeller, H., Katic, I., Pedersen, P.H., Markussen, W.B., 2019. Comparison of compressor control strategies for solar direct drive refrigerators. In Proceedings of the 25th IIR International Congress of Refrigeration, August 24-30, Montreal, Canada

Klein, S.A., 2018. Engineering equation solver academic professional v10.478.

Pedersen, P.H., Katic, I., Markussen, W.B., Jensen, J.K., Cording, C., Moeller, H., 2019. Direct drive solar coolers. In Proceedings of the 25th IIR International Congress of Refrigeration, August 24-30, Montreal, Canada

Pilatte, A., 1984. A photovoltaic refrigerator for storage of vaccines and icemaking. In Energy for Rural and Island Communities. In Proceedings of the Third International Conference Held at Inverness, Scotland, pages 229-237. Elsevier.

Walker, C.D., 2007. Design and manufacture of low cost vaccine cooler. PhD thesis, Massachusetts Institute of Technology, 2007.

Wang F.J., Chang J.C., Lin K.C., Yau, Y.H., 2011. Performance testing of a thermoelectric cooler for medical application. In Advanced Materials Research 255,1537-1540.

WHO, 2010, Refrigerator or combined refrigerator and water-pack freezer: compression-cycle. Solar direct drive without battery storage, PQS Independent type-testing protocol, E003/RF05-VP.2

World Health Organization, 2015. Immunization in practice: a practical guide for health staff, 2015 update. World Health Organization. http://www.who.int/iris/handle/10665/193412

World Health Organization, 2018. Immunization coverage. http://www.who.int/mediacentre/factsheets/fs378/en/, last visited January 31, 2019.